



since 1961

**Baltica**

*BALTICA* Volume 27 Number 1 June 2014 : 33–44

doi: 10.5200/baltica.2014.27.04

## Testing and numerical simulation of Holocene marine sand uniaxial compression at Lithuanian coast

*Šarūnas Skuodis, Darius Markauskas, Arnoldas Norkus, Gintaras Žaržojus, Neringa Dirgėlienė*

Skuodis Š., Markauskas D., Norkus A., Žaržojus G., Dirgėlienė N., 2014. Testing and numerical simulation of Holocene marine sand uniaxial compression at Lithuanian coast. *Baltica*, 27 (1), 33–44. Vilnius. EISSN 1648-858X.

Manuscript submitted 29 January 2014 / Accepted 5 May 2014 / Published online 9 June 2014

© *Baltica* 2014

**Abstract** Compressibility of quartz sand from the Lithuanian coastal area in Klaipėda environs is investigated by testing and numerical simulation, with validation of obtained results. The shape of sand grains has been analysed with a scanning electronic microscope (SEM). The determined morphological parameters of sand grains are employed to create discrete models (particle models of grains) subsequently used for sand compression test numerical simulation via discrete element method (DEM) techniques. The background version of DEM and the numerical time-integration algorithm are implemented in original DEMMAT code. Compression tests have been realised by an oedometer device. Test versus numerical simulation results have revealed a dependence of significant compression curve character on the discretised shape of sand grains and Young's modulus of particles.

**Keywords** • oedometer • sand • uniaxial compression • morphological parameters • numerical simulation • discrete element method

✉ *Šarūnas Skuodis (sarunas.skuodis@vgtu.lt), Darius Markauskas, Arnoldas Norkus, Gintaras Žaržojus, Neringa Dirgėlienė, Vilnius Gediminas Technical University, Saulėtekio al. 11, LT-10223 Vilnius, Lithuania*

## INTRODUCTION

Evaluation of the actual compressibility properties via soil compression tests is important for employment of subsequent numerical analysis of stress and strain state of ground subjected by supplement loading (e.g. loads transmitted via foundations from a superstructure, interaction of structure and soil strata, etc). The confined compression (oedometer) test is approved as a relatively fast and simple laboratory test. It is performed under different conditions, loading paths and durability. Test conditions depend on physical changes of multiphase system of soil, generally related with reorganisation of soil grains, that of initial change of skeleton in cohesive soils and velocity of water filtration in saturated soils. One must note that in some cases the duration of testing procedure for prediction of long term soil behaviour and in other specific cases is very long (Tong, Yin 2011), thus sometimes taking into account the time and test cost ratio it is not worth even to start the test. From the other hand one cannot qualitatively explain the variation of soil compression test results, basing on some processing of already known testing and analysis

data separately or in concert with a view analysis. It is obvious, that having not identified the actual physical mechanism for soil grain reorganisation during compression process and its peculiarities, one cannot explain the observed scatter of test results under disposal. This mechanism cannot be recorded by applying usual techniques of testing and view analysis but can be simulated applying the relevant discrete element method (DEM) techniques, employed mathematical models of processes and the discrete models of soil grains.

The above-mentioned circumstances as well as the permanently reducing computational costs, the development of numerical techniques and software in the field of multi-scale analysis (including the particle strata mechanics) initiated a fast development and the applications in the field of the soil behaviour numerical analysis by means of DEM. Such an approach combined with an experimental analysis for validation and calibration of the mathematical models is definitely a promising one, allowing reduce the price and quantity of laboratory tests and a reasonless conservatism in determining the design values of mechanical properties of soils in near future.

Currently, one can find many research reports on sand compression tests accompanied by numerical modelling of the tests for soil in order to reproduce the soil compression nature (Singh *et al.* 2012; Berg, Johannsmann 2003; Lewandowska, Pilawski 2012; Vittorias *et al.* 2010). However, one faces with many difficulties as particle shape discretization, problem size, singularity, convergence and many other difficulties, which appear in numerical simulations using DEM (Cavarretta 2009; Luding 2008; Khanal, Tomas 2008; Zhu *et al.* 2008).

It is obvious that evaluation of 3D versus 2D models of compression test is much more efficient and exact. Generally, one deals with technical difficulties and amount of time, relevant technical resources and skills to evaluate 3D model of sand grains.

Therefore, a rational approach for saving time in discretisation of sand grains, that of computational resources and simulation accuracy requires substantiate the relevant morphology investigation via image analysis method, namely: using either the three dimension (3D) approach if it is rather irregular in volume, or two dimensions (2D) one, otherwise. The investigated sand samples correspond the Baltic Sea coast sand in Klaipėda environs (generally typical sand for Baltic Sea coast) with grains of high enough natural sphericity, roundness and roughness. Thus, 2D analysis is sufficient approach as 2D and 3D morphology parameters are very similar.

Another principal approach and discussion is related with the aspects and simplifications of numerical modelling via DEM processes. The state of art in the field of investigations, aimed for decreasing the computational time via DEM techniques (Fakhri *et al.* 2012), summarise the following, namely: (a) diameter sand grains is increased (Renouf *et al.* 2006); (b) Young's modulus of particles is decreased or taken natural as for quartz (Yohannes *et al.* 2013; Lim, McDowell 2008); (c) density of particle is artificially increased (Tordesillas *et al.* 2009); (d) the soil grading curve different from that obtained via test is employed for simulation of soil grain size distribution (Arasan *et al.* 2011); (e) the soil sample size and/or size of grains are reduced (Wu *et al.* 2009; Prisco, Galli 2011; Calvetti 2008) or the sample and grains sizes are increased (Geng *et al.* 2012; Chen, Zhou 2012); (f) discrete model of actual grain shape is simulated either as a simple sphere (Lin, Wu 2012; Safronov *et al.* 2012; Jasevičius *et al.* 2011; Abbas *et al.* 2005; Markauskas, Kačianauskas 2006) or as a multisphere (Tumonis *et al.* 2012; Kruggel-Emden *et al.* 2008); (g) soil is simulated omitting the smallest grains (particles) (Modenese *et al.* 2012).

The compressibility of Klaipėda environs sand samples is analysed via testing, numerical simulation, subsequent validation of obtained results is per-

formed. The aim of the present paper is to evaluate numerically the actual reorganisation of soil particles during compression process. Validation criterion is a response of the sample to be compatible with that recorded via the testing. The following techniques (from the above listed ones) for this purpose are employed, namely: creating of the discrete models of soil grains based on scanning electronic microscope (SEM) 2D view morphological analysis; simulating the grading curve of the soil to be compatible with an actual one; choosing the different physical parameters of soil grains and oedometer device, reducing in proportion (versus actual test) the composition and the number of particles for numerical simulation; and reducing in proportion the time of simulation in the way to avoid dynamic effects.

## ENGINEERING GEOLOGICAL SETTING

The sediments deposited on the Lithuanian coast of the Baltic Sea have been formed during the Quaternary. There are two geologically and geomorphologically different sectors of the Lithuanian coastal area: the mainland area (to the north from Klaipėda) and the Curonian Spit [Kuršių Nerija] (Gudelis 1992). The investigated area is located in the southern part of the Lithuanian mainland area of the Baltic Sea (the northern part of Klaipėda city) (Fig. 1).

Northwards from the Klaipėda city, only the immediate near coast area contains a sandy strip of Holocene marine sediments (m IV), which occur as deep as to 4–5 metres in the sea. The material composing the near shore sediments mainly consists of different sand, where medium coarse and fine sand (Repečka 1999; Gulbinskas, Trimonis 1999) with admixture of gravel and organic matter (Gadeikis, Repečka 1999; Dundulis *et al.* 2006) prevails. This sand has been used for investigations (one sample of 14 kg). The coordinates of sampling location (marked in Fig. 1) are 55°46'4.07", 21°4'39.06" (WGS), and sampling depth 0.4–0.5 metres.

The average density of particles ( $\rho_s$ ) for marine sands is 2.67 Mg/m<sup>3</sup> and varies from 2.65 to 2.71 Mg/m<sup>3</sup>, respectively. The bulk density of the sand varies from 1.83 to 2.09 Mg/m<sup>3</sup>, where the average is 1.98 Mg/m<sup>3</sup>. Regardless of the genesis of marine sand and their grain size distribution, quartz and feldspar prevail in mineral composition. The natural moisture content ( $w$ ) depends on a degree of saturation and ranges from 13.7 to 27.7%. The void ratio ( $e$ ) in fine sand varies from 0.474 to 0.778 (Gadeikis, Repečka 1999; Dundulis *et al.* 2004; Dundulis *et al.* 2006). The recent marine sediments (m IV) have been formed in the coastal zone, therefore high sphericity  $P = 0.84$  (Dundulis *et al.* 2004) is a distinctive morphological feature of grain shape.

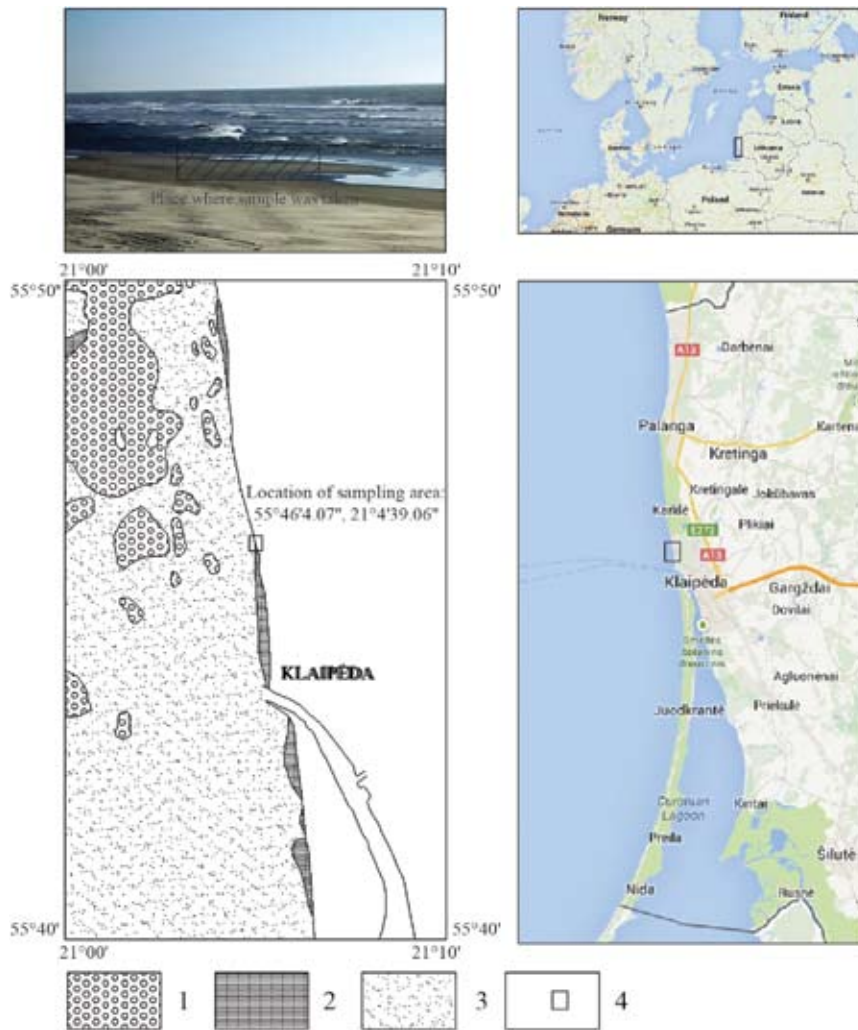


**Fig. 1** Location of investigated site and lithological types of bottom surface sediments (after S. Gulbinskas and E. Trimonis 1999): 1 – boulders (>64 mm) and gravel (64–2 mm); 2 – coarse-grained (2–0.5 mm) and medium-grained (0.5–0.25 mm) sand; 3 – fine sand (0.5–0.063 mm); 4 – location of investigation area.

## EXPERIMENTAL SETUP

### Evaluation of sand morphological parameters

The mineralogical composition of sand under investigation was determined by Amšiejus et al. (2010), where sand is found to contain ~85 % quartz and ~6 % feldspar with remaining contribution of carbonate, mica and some other minerals. The sand sieving test (Fig. 2) has been performed to identify the governing fractions for evaluation of morphological parameters via scanning electronic microscope (SEM) analysis and the subsequent creation of discrete models of sand grains.

Fig. 3 presents the identified and further investigated fractions of grains with SEM: the panoramic view in the top picture and the magnification of 2.00–1.18 mm sand fraction (corresponding the marked area in panoramic view) in the bottom picture. Note that smaller fractions within the 0.0063–0.15 mm are omitted in the panoramic view as due to the lack of place for picturing.

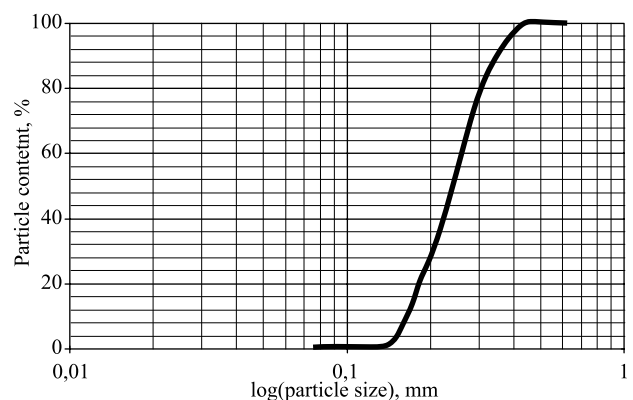


**Fig. 2** Soil grading curve according to LST EN ISO 14688-2:2007.

The main morphological parameters for 2D view analysis of sand grains are as follow (Kavrus, Skuodis 2012; Prušinskienė 2012):

- area, mm<sup>2</sup>;
- equivalent diameter, mm;

- sphericity;
- circularity;
- form coefficient;
- angularity.

33 different sand grains, corresponding basic nine sand fractions (according to LST EN ISO 14688-2:2007) have been examined, the total number of examined grains being 297. Morphological parameters

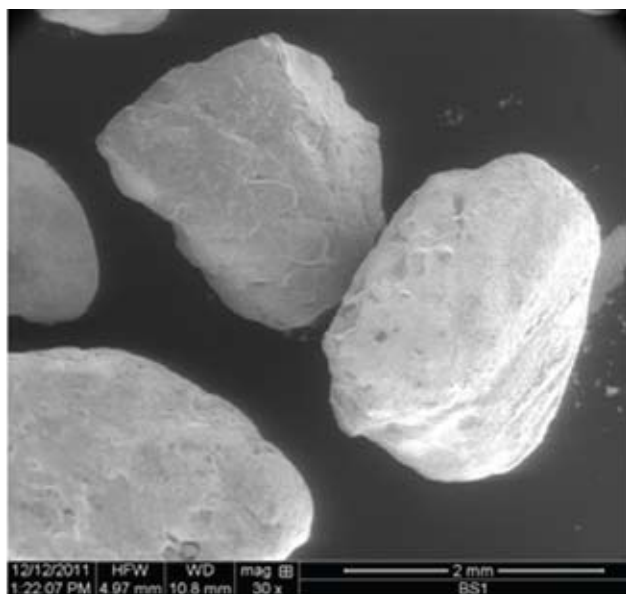
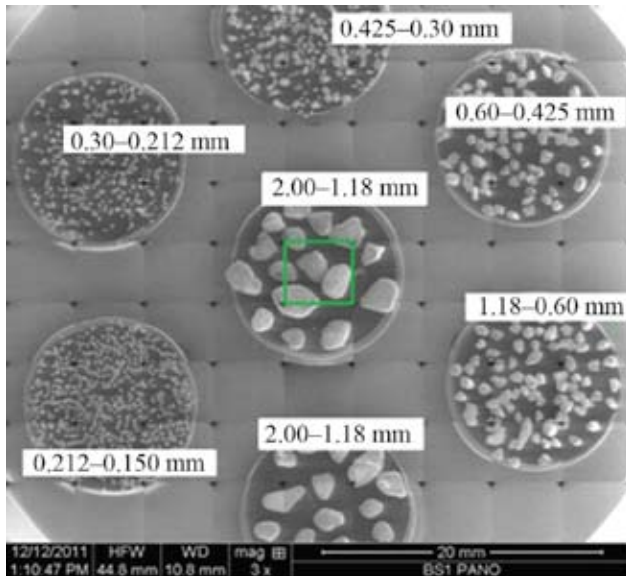


**Fig. 3** Soil 2D investigation with SEM: pictures of panoramic view (top) and magnification of marked area (bottom).

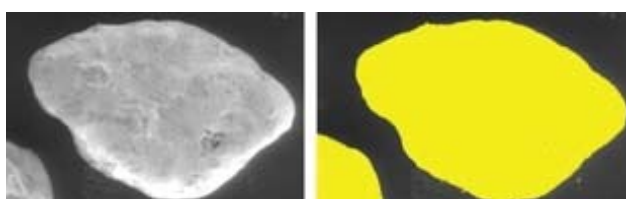



**Fig. 4** Actual (left) and computed (right) 2D morphological parameters with STIMAN (Kavrus, Skuodis 2012).

calculated applying the specialised software STIMAN (STIMAN 2010). The input data for the calculation program of STIMAN are the views of pictures (Fig. 4) that determines the selected morphological parameters according to the developed algorithm. Such direct automatic sequence: view analysis processing – preparing input data – calculation – output of determined parameters, ensures the accuracy of obtained values (Allonso-Marroquin 2008; CEGEO *et al.* 2012) as it is not necessary to apply any additional calculations (Blott, Pye 2008; Charpentier *et al.* 2013; Roussillon *et al.* 2009; Montenegro *et al.* 2013; Tafesse 2013) for determining the final magnitudes of investigated morphological parameters.

The morphological parameters have been determined for all grains of selected sand fractions. An analysis of the determined morphological parameters within each fraction has shown that the shape of all grains is rather similar, i.e. the grains differ principally only in size. Therefore, in the case of analysed sand sample it is sufficient to create the single generalised (typical) shape discrete model of a particle of different sizes in fractures.

A development of the discrete model for the typical shape particle requires determine the mean morphological parameters. The obtained mean 2D morphological parameters of the particle are given in Table 1.

**Table 1** Mean morphological parameters (2D case). Compiled by Š. Skuodis 2013.

Morphological parameter	Mean value
Area (mm <sup>2</sup> )	0.1122
Equivalent diameter (mm)	0.340
Sphericity	0.836
Circularity	0.515
Form coefficient	0.702
Angularity	0.410
Particle shape	

The mean shape (Table 1) of investigated sand grain has been determined using Krumbein and Slos (1951) and Cho *et al.* (2006) given solutions for sand shape characterisation according to the particle sphericity and roundness. In this case, it is not necessary to use Fourier descriptors (Mollon, Zhao 2013).

### Sand compression test

The air-dry sand samples have been prepared for experimental analysis (oedometer test). The compression tests have been performed by the universal oedom-



**Fig. 5** Universal oedometer apparatus ADS 1/3 (Wille Geotech Group, 2010).

eter apparatus ADS 1/3 (Wille Geotech Group 2010; Fig. 5). The oedometer volume is of a cylinder form, its height is 3.39 cm and diameter is 7.14 cm.

Aiming to approach the initial soil states (conditions) for compression test and its numerical simulation, the filling of the oedometer volume (sampling) in both cases has been realised via free fall way of sand grains (particles for DEM analysis): the sand has been poured in volume via free fall from 15 mm height above the top of the oedometer ring. Such sampling technique for physical test resulted the maximal initial void ratio  $e_o = 0.784$ .

The applied sample vertical loading ramp is 400.0 kPa/min. The loading velocity in this case has no influence (no dynamic effects recognised) for soil compression results as it is within the bounds of 25.0 to 800.0 kPa/min leading to the similar processing of sand compression curve (Skuodis *et al.* 2013). The applied maximum vertical stress on top of the sample is 400.0 kPa, resulting the final vertical strain  $\varepsilon = 1.76\%$  at the end of compression process. Compression testing data have been recorded by  $\sim 0.5$  s time intervals.

## DEM SIMULATIONS

DEM treats each constituent of composite particle as a separate entity. The entities are considered as distinct elements, the motion and material constitutive laws are applied to each element. The DEM methodology, which was initiated by P. Cundall and O. Strack (1979), allows reproduce an interactions between particles and that of between their physical

environment (e.g. contact between particles parts of oedometer volume).

The current work presents the application of DEM techniques for the analysis of sand compression process. The background version of DEM and the numerical time-integration algorithm were developed and implemented into original DEMMAT code. The quality of implementation is handled by a physically observable behaviour of interactions: particle-particle, particle-wall, particle-bottom and/or top plate, and by the validation with the results obtained from physical experiments. More detailed information about DEMMAT code is given in Balevičius *et al.* (2004).

The main reason of choosing DEMMAT code to simulate the soil compression tests is a possibility to run calculations in a cluster (<http://www.vilkas.vgtu.lt>). The cluster ensures an employment of large computational capacities, necessary to simulate the 3D compaction processes in particular. When using the cluster, the oedometer volume filled by simulated particles is separated into four pieces, and the calculations are performed by separate computers corresponding the each piece (Fig. 6). When a particle during compaction (i.e. repositioning) process moves from one neighbour piece to another one, then all the calculations corresponding the particle are done by the another computer. For this reason, all computers at each time step are calculating different quantities of particles.

Three different particle shapes (soil grain subscribed as sphere (S), soil grain subscribed with 2 spheres (MS2), soil grain subscribed with 3 spheres (MS3)) to reproduce the sand sample have been employed for simulations (Fig. 7) aiming to investigate the influence of morphology parameters for approaching the actual compression process to the one obtained via testing. Three samples from the above listed mean shapes have been numerically generated to correspond the obtained soil-grading curve (Fig. 8) to match the one obtained via sieve test of investigated soil.

The test process and parameters for simulations are presented in Table. 2. The actual Young's modulus  $E_{oed} = 200$  GPa for oedometer volume parts is



**Fig. 6** An example of simulation process with cluster.

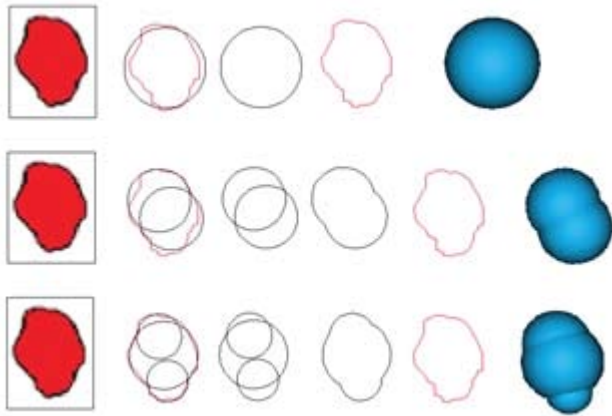


**Fig. 7** Reconstruction of particle shapes according to mean 2D particle shape.

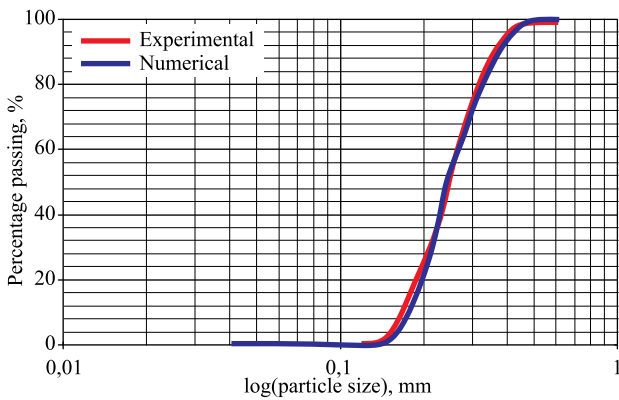


**Fig. 8** Soil experimental and simulated grading curves.

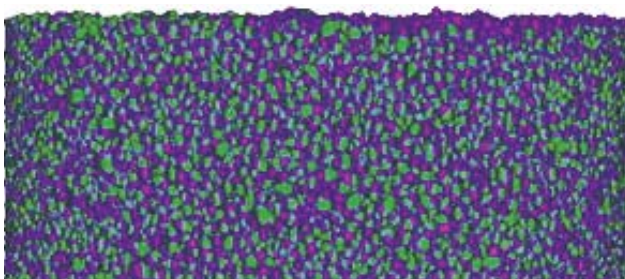


**Fig. 9** Comparison of simulation using different particle properties: green particle ( $E_p = 10$  MPa,  $\rho_s = 2650$  kg/m<sup>3</sup>) and purple particle ( $E_p = 78000$  MPa,  $\rho_s = 2650000$  kg/m<sup>3</sup>).

employed for simulations. The volume of oedometer is scaled/reduced in proportion to the employed one for the experimental tests, aiming to reproduce similar conditions and the nature of compaction process. The scaling is necessary to reduce the quantity of particles, i. e. to reduce the computational time, which even for cluster was relatively large (varied within 240–480 hours per performed simulations). The increment of the density of particle (Table 2) results a reduction of the soil simulation with DEM. Fig. 9 illustrates that a huge mass of the single particle does not affect the magnitude of sample void ratio obtained via numerical generation of sample. In this case, the first Newton law of motion (Bogdanovičius 2010) is

**Table 2** Test model data\*. Compiled by Š. Skuodis and D. Markauskas, 2013.

Quantity	Symbol	Unit	Numerical simulation
Solid density	$\rho_s$	kg/m <sup>3</sup>	2650; 2650x10 <sup>3</sup>
Void ratio	$e$	–	0.512
Elasticity modulus of particle	$E_p$	MPa	10; 78000; 98000
Number of particles	$n$	–	30846 (MS3); 38923 (MS2); 46095 (S)
Friction coefficient particle–particle	$\mu$	–	0.84
Friction coefficient particle–wall	$\mu$	–	0.3
Friction coefficient wall–wall	$\mu$	–	0.3
Rolling friction	$\mu_{rol}$	–	0.04
Time step	$\Delta t$	s	$2 \times 10^{-7}$ ; $5 \times 10^{-7}$
Contact law	–	–	Hertz
Loading velocity	$v$	m/s	0.000484284
Strain	$\varepsilon$	%	1.76
Oedometer height	$h$	m	0.00484
Oedometer diameter	$d$	m	0.0102

\*Note: several values in column 4 correspond to the parameters for separately simulated cases.

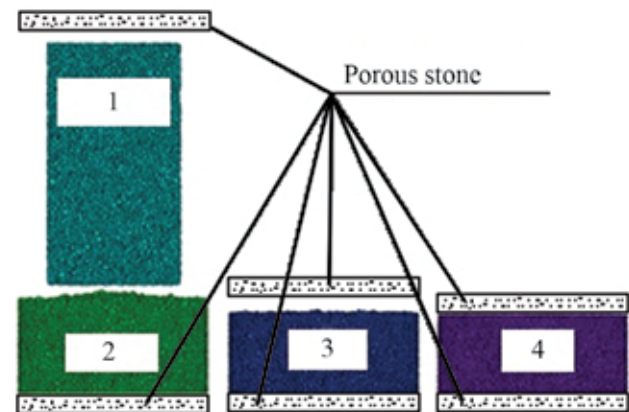


**Fig. 10** Stages of numerical simulation of compaction: 1 – generation of random particles; 2 – oedometer filling; 3 – sample surface flattening; 4 – compression of sample.

valid. The wall–wall friction coefficient is activated only when walls of oedometer device are in contact with porous stone. It is assumed that oedometer walls and porous stone have no interaction.

The stages required to perform numerical simulation of compaction process are presented in Fig. 10.

The stages 1–3 are the preparatory ones, each requiring time-consuming stage-by-stage solutions of complex problems. Note that the stage 1 results random position and orientation of particles. The surface flattening is simulated by deleting the unnecessary particles. The heights of samples of stage 3 and stage 4 differ insignificantly as compressions process yields small strain magnitude of 1.76 % (the same as in physical test). The vertical stress applied on top of porous stone is computed by dividing the sum of contact normal forces to the area of porous stone.

## RESULTS

The influence of scaling factor via different magnitudes of Young's modulus ( $E_p$ ) of particles to simulate the compaction curve (reaching the same vertical strain magnitude of 1.76 % obtained by experimental test) has been analysed via performed simulations. As for example, Fig. 11 shows DEM simulation process of sample compression using discrete model of particles, created from three spheres (MS3) for  $E_p = 10$  MPa. One can find in Fig. 11 that vertical stress (of top porous stone)  $\sigma = 1.93$  kPa is very small to reach the same strain magnitude as in physical experiment (corresponding  $\sigma = 400.0$  kPa. Despite the good matching of the compression curve with the experimental test, one must emphasize that it does not reproduce the actual process, i.e. the nature of reorganisation of particles during compaction process. An analysis of the simulated process yields that particles have a very high overlap (mean particle overlap is  $\varepsilon = 5.28 \cdot 10^{-6}$  m) on each other during compaction.

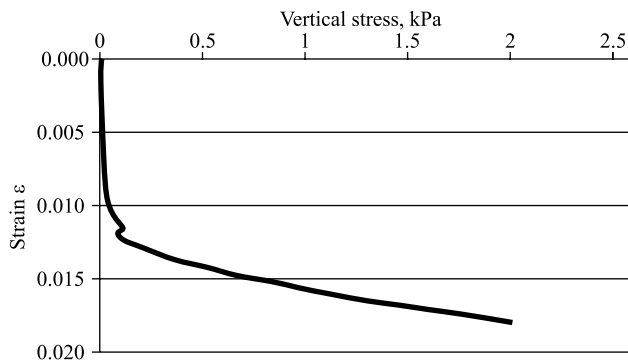


**Fig. 11** Vertical stress versus strain, soil of MS3 particles ( $E_p = 10$  GPa).

Therefore, it corresponds a case of large elastic deformations and a small amount of rearrangements that is in contrary of actual compaction processes prescribed in principal by a repositioning of particles and only infinitesimally small elastic deformations of particles. This, as well as many other performed numerical simulations for other magnitudes, has yielded that applications of  $E_p$

below 10.0 MPa in concert with the relevant reduced loading stress magnitude is essentially time consuming, problematic, and non-efficient and the hardly handled approach aiming to “catch” the nature of the actual compaction process via repositioning of particles.

The identified minimum magnitude of Young's modulus for single particle is  $E_p = 78.0$  GPa. This magnitude ensures only infinitesimally small overlaps of particles during compaction process. The vertical strain magnitude of 1.76 % is reached for vertical stress  $\sigma = 327.03$  kPa for this magnitude, versus the 400.0 kPa corresponding the experimental test one (the difference comparing with test is 18.2 %). The compaction curve for this case is presented in Fig. 12.

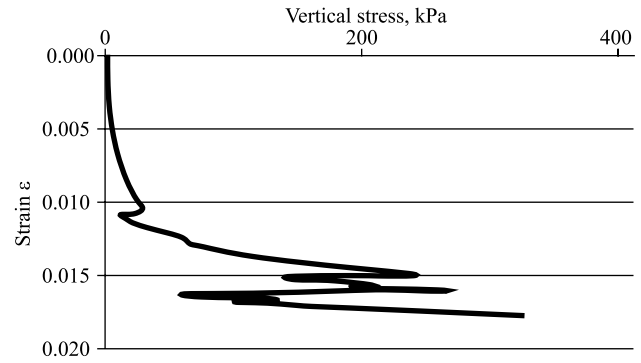


**Fig. 12** Vertical stress versus strain (MS3,  $E_p = 78$  GPa).

The analogous simulations of soil compaction have been performed also for larger  $E_p$  magnitudes. The view of compaction curve for the actual Young's modulus of particle  $E_p = 78.0$  and 98.0 GPa, is presented in Fig. 13. The criterion for choosing the 78.0 or 98.0 GPa magnitudes is based by the reference ([www.almazoptics.com/Quartz.htm](http://www.almazoptics.com/Quartz.htm)) where given for quartz the Young's modulus are 76.5 GPa and 97.2 GPa for perpendicular directions, respectively. The constant isotropic parameter versus anisotropic parameters of elasticity modulus has been chosen for the reason that it has no principle influence for repositioning process of particles.

Simulation of the compaction process for fixed strain magnitude ( $\varepsilon = 1.76$  %) and  $E_p = 98.0$  GPa, has resulted the vertical stress  $\sigma = 374.31$  kPa, that is 6.4 % less than the obtained one from experimental test. Note, that almost no overlap between particles for both magnitudes of  $E_p$  is identified, they correspond the vertical stress magnitudes, close to each other and to the test one. One must also keep in mind that numerical simulation represents an ideal and scaled model of sample, while the testing device load distribution method to sample, the actual rigidity of parts and the measurement method also contributes some inaccuracy in determining of exact values.

Only after when the magnitudes of  $E_p$ , ensuring the actual compaction process are identified, one can

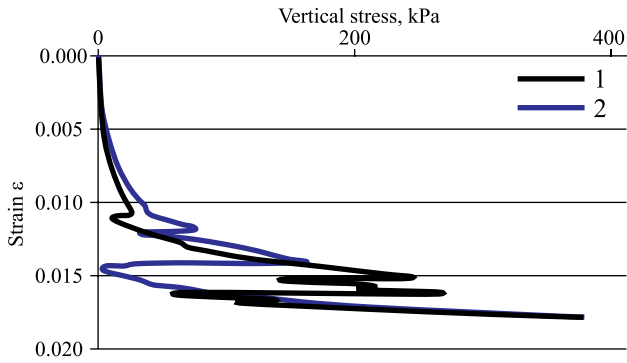


**Fig. 13** Vertical stress versus strain: 1 – MS3,  $E_p = 78.0$  GPa; 2 – MS3,  $E_p = 98.0$  GPa.

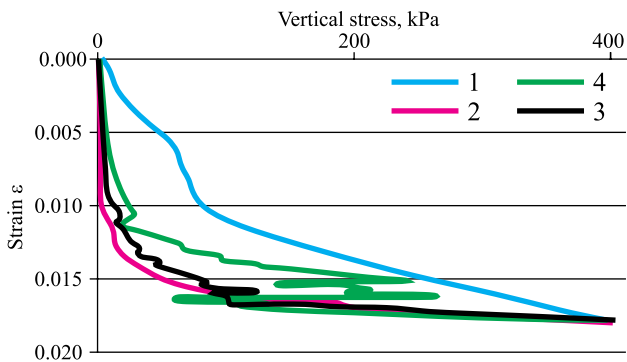


**Fig. 14** Vertical stress versus strain curves of experimental test (1) and simulated ( $E_p = 78.0$  GPa) for spherical (2), 2–sphere (3) and 3–sphere (4) discrete models.

investigate the influence of particle shape aiming to obtain the compaction curve close to that of the test. Fig. 14 presents the compaction curves from test (experiment) one and the simulated ones for  $E_p = 78$  GPa for three different discrete models of particles (see Fig. 7), namely: sphere (S) particles, 2 sphere (MS2) particles and 3 sphere (MS3) particles.

One can find that the shapes of compaction curves, including the stress jumps observed in Figs. 12–14, corresponding to the test and the numerical simulation results differ, but they all lead to the same strain magnitude at the end of compaction process. Note, that simulated compaction time is not actual (as in test), but scaled for reducing computational resources.

The magnitude of elasticity modulus of particle  $E_p$  influences the velocity of repositioning of particles. The cases of  $E_p = 78.0$  GPa and  $E_p = 98.0$  GPa have been analysed. The repositioning process of particles of a higher elasticity modulus ( $E_p = 98.0$  GPa) is faster than that for less stiff particles ( $E_p = 78.0$  GPa). When a repositioning velocity of particles is faster than that of the porous stone (transmitting the top loading stress to sample), it results the stress jumps recorded by simulated compaction curve. An example of this phenomenon for a single particle is illustrated in Fig. 15. The jumps usually appear until the assembly of all particles goes to a final repositioning. The repositioning dis-

tance of particles is very small comparing with the one for the vertical stress magnitudes above  $\sim 200$  kPa, id. est. after a major reduction of void volume in previous loading stages. One must note that the stress jumps can be recognised also in experimental testing. However, these stress jumps are not so dramatically high, because loading velocity of porous stone of oedometer (the pressure increment velocity is constrained due the technical capacities of device) is much lower than the one realised via numerical simulation.

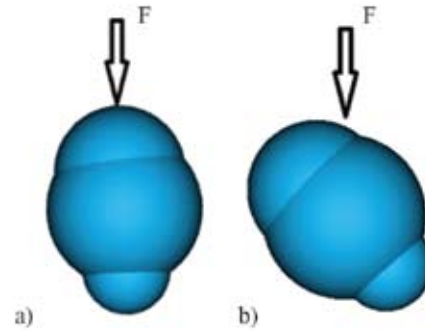


**Fig. 15** Repositioning phases: (a) particle is in contact with force (F) established by porous stone; and (b) temporary gap between porous stone and new particle position.

A more detailed description of the observed stress jumps in simulated compaction curves (see Fig. 13) is presented below for the case of MS3 particles of  $E_p = 98.0$  GPa (Fig. 16). Find that the stress jump appears for the strain  $\varepsilon \sim 0.014$ . That means that repositioning of particles is very high at this strain. The view of reorganisation of particles of compaction process via the vectors of velocities for strain increments, corresponding the 3-time step calculations for strain magnitudes  $\varepsilon = 0.01385$ ;  $0.01391$  and  $0.01396$  (i.e. in vicinity of  $\varepsilon \sim 0.014$ ) are given in Fig. 17.

One can find from Fig. 17 that major repositioning of particles is observed near the top of sample (main concentration of velocity vectors). A small quantity (volume) of the particles was cut from simulated oedometer test sample for more detailed investigation of repositioning of particles. The repositioning of particles of this volume (Fig. 18) has been analysed for three different strains at the stress jump vicinity (see Fig. 16 and 17).

Having performed the analysis of views in Fig. 18, one can conclude, that the main repositioning amount is in vicinity of the top of a sample, and less amount of repositioning of particles (especially of larger size ones) is detected per remaining height of sample. One can state that all sample particles work as an assembly. Even if only few particles change this position, it causes the subsequent reorganisations of all remaining particles. The character of repositioning process has a high influence for total vertical stress magnitude on top of the sample. One must note that quantity of



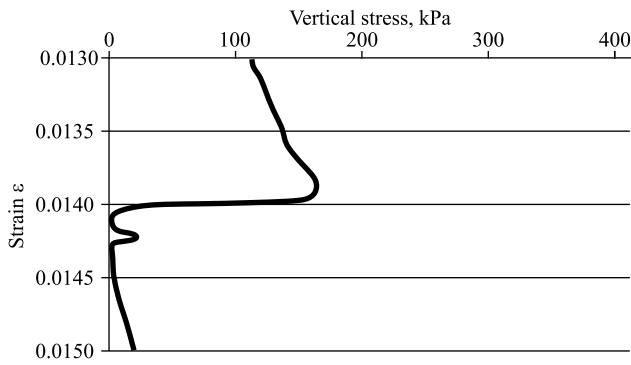


**Fig. 16** Stress jump detailing during compression simulation.

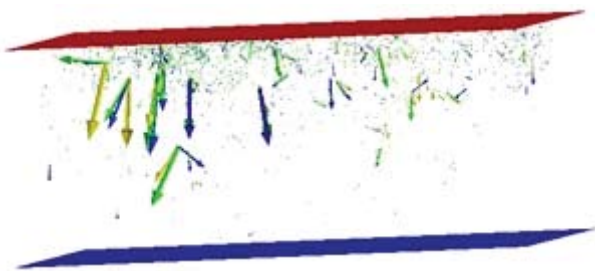


**Fig. 17** Velocity vectors: green  $-\varepsilon = 0.01385$ ; blue  $-\varepsilon = 0.01385$ ; yellow  $-\varepsilon = 0.01385$ .

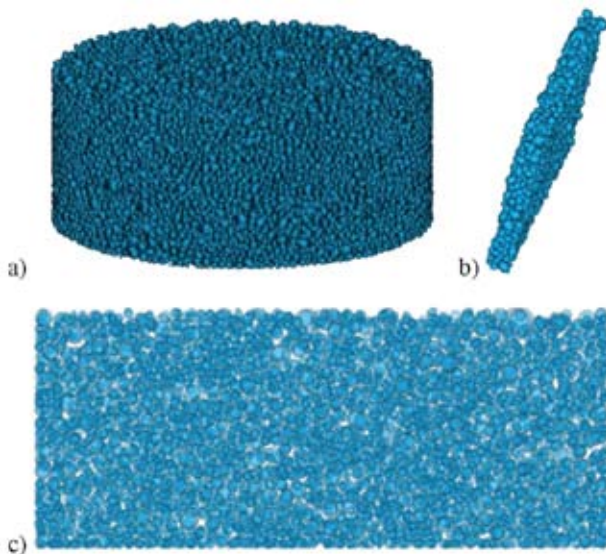


**Fig. 18** Simulated repositioning of particles at the different strains: (a) all simulated particles of oedometer sample; (b) cut out small volume of particles of oedometer sample; and (c) cut out particles repositioning at the stress jump when  $\varepsilon = 0.01385$ ; 0.01391 and 0.01396.

particles has a significant influence on the simulated vertical stress magnitude on top of the sample and on the character of reorganisation of particles as well. Therefore, ten rows of particles of sample height were found to be a minimum one for the analysis of the compaction nature.

Discretization of sand grain by maximum three spheres is compatible only from 2D view morphology analysis results. If the grain discrete model is created from larger number of spheres, e. g. five spheres,

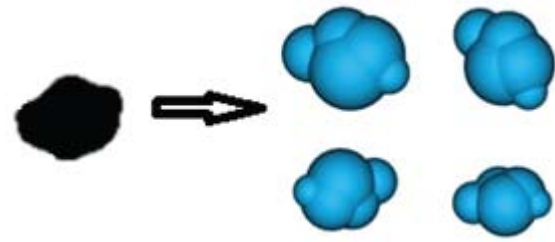


**Fig. 19** Particle shape reconstruction.

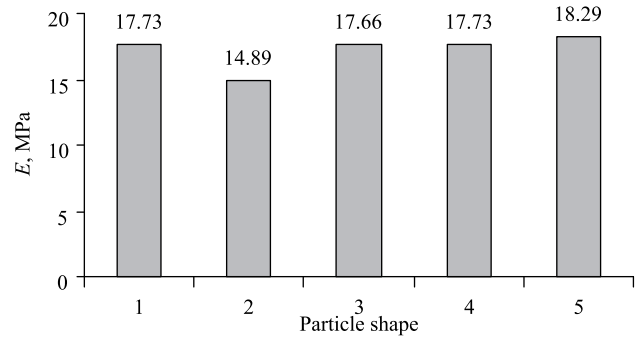


**Fig. 20** Deformation modulus from test and simulations results: (1) experimental test; (2) MS3 of  $E_p = 78$  GPa; (3) MS3 of  $E_p = 98$  GPa; (4) Spherical particle of  $E_p = 78$  GPa; and (5) MS2 of  $E_p = 78$  GPa.

the particle shape conforms only one projection (2D model), while in other projections (3D model) the shape will differ (Fig. 19).

The deformation modulus  $E$  of a soil sample can be calculated from the stress–strain curve. The secant soil deformation modulus has been calculated using the formula:  $E = (\Delta\sigma/\Delta\varepsilon)\beta$ , where  $\beta$  for sand is equal to 0.8 (Statkus, Martinkus 2013). Comparison of secant deformation modulus magnitudes calculated from compaction curves are given in Fig. 20. The results given in Fig. 20 clearly show, that particle shape has small influence for secant soil deformation modulus in case of high magnitude of Young's modulus ( $E_p = 78$  GPa) of particle. However, in separate cases when eg. the process of deformation (variation of deformation modulus  $E$  versus different stages of loading) is necessary for considering, one must choose more complex discrete model of particle to reproduce the actual stress-strain curve (see Fig. 14).

## CONCLUSIONS

The numerical simulation of sand compressibility via DEM techniques is powerful and efficient method. It should be emphasised, that actually it is the only available tool to reproduce and describe the mechanism of actual processes for granular strata, so far. It allows identify proper soil response values employed in engineering practice. However, it requires deep knowledge and skills in geotechnical engineering, DEM modelling, laboratory testing, analysing and validating of the obtained results for identifying the

governing factors, conditioning the nature of compressibility. These factors can be divided into two groups, namely: first, those related to soil behaviour and second, those related to testing and measurement procedures and inaccuracies/peculiarities of testing and numerical modelling.

The current research concentrated on detailed investigation of several of the factors met in both groups, their contribution in modelling of the compaction process. The main findings, conclusions and future trends and perspectives are listed below:

The influence of discretised shape of particles is less sensitive versus Young's modulus of particle for determining the soil secant deformation modulus. For determining the magnitudes via DEM close to the test one, one must employ the large magnitudes of Young's modulus of particle, approaching the actual one ( $E_p = 78\text{--}98$  GPa). In this case, simulation time increases significantly, comparing the reduced (scaled) one, but it ensures the actual repositioning of particles during compaction process.

A simultaneous "fictitious" increment of particle density and keeping the real Young's modulus of particle is amongst the tools to save the computational resources. It allows an escaping of high overlapping (id. est. large elastic deformations of separate particles), which are not met in the actual compaction process.

One cannot arbitrarily reduce the number of particles aiming to save computational resources, as the actual interaction of soil sample with oedometer volume (boundary conditions) as well as the reorganisation of particles could be not relevant for reproducing the test. The "rational" minimal member of particles for simulation could be a trend for further investigations.

The discrete models of sand grains were created basing on 2D SEM view analysis. This approach, reducing the efforts, comparing with that of 3D analysis is not general, but sufficient in investigated case as related with "quite regular" natural shape of typical Klaipėda environs sand grains. Surely, the analysis of other types of sand grains could lead for necessity of 3D view analysis and the necessity of creation of discrete models of particles from larger number of spheres. An employment of multi-spherical particles increases significantly computational resources; therefore, possibilities to reduce them should be analyzed and properly validated with the tests, e.g. applying smaller number of spheres for creating discrete model of particle in concert with a relevant "correction" of friction properties and/or applying other techniques. This approach also can be perspective for further investigations.

The influence of the creating discrete models for each fraction versus the mean one for all fractures

should be investigated in future. Due to experience of authors, the peculiarities of testing device, both in transmitting the loading to soil sample, gaps, rigidity of device parts, measurement peculiarities, etc. also contribute the accuracy of testing, therefore should be evaluated in mathematical model of the process. The influence of the above-mentioned factors, contributing the accuracy of numerical modelling is a future trend.

### Acknowledgements

The authors express their gratitude to Dr. Lumir Mica (Brno), Dr. Krzysztof Szarf (Gdańsk) and Dr. Petras Šinkūnas (Vilnius) for useful remarks and valuable comments made on the manuscript. The equipment and infrastructure of Civil Engineering Research Centre of Vilnius Gediminas Technical University were employed for this investigation.

### References

- Abbas, A., Masad, E., Papagiannakis, T., Shenoy, A., 2005. Modelling asphalt mastic stiffness using discrete element analysis and micromechanics-based models. *International Journal of Pavement Engineering* 6 (2), 137–146. <http://dx.doi.org/10.1080/10298430500159040>
- Amšiejus, J., Kačianauskas, R., Norkus, A., Tumonis, L., 2010. Investigation of sand porosity via oedometric testing. *The Baltic Journal of Road and Bridge Engineering* 5 (3), 139–147. <http://dx.doi.org/10.3846/bjrbe.2010.20>
- Allonso-Marroquin, F., 2008. Spheropolygons: A new method to simulate conservative and dissipative interactions between 2D complex-shaped rigid bodies. *EPL (Europhysics Letters)* 83 (1), 14001. <http://dx.doi.org/10.1209/0295-5075/83/14001>
- Arasan, S., Akbulut, S., Hasiloglu, A. S., 2011. Effect of particle size and shape on the grain size distribution using Image analysis. *International Journal of Civil and Structural Engineering* 1 (4), 968–985.
- Balevičius, R., Džiugys, A., Kačianauskas, R., 2004. Discrete element method and its application to the analysis of penetration into granular media. *Journal of Civil Engineering and Management* 10 (1), 3–14. <http://dx.doi.org/10.1080/13923730.2004.9636280>
- Berg, S., Johannsmann, D., 2003. Nonlinearities in contact mechanics experiments with quartz crystal resonators. *Surface Science* 541 (2003), 225–233. [http://dx.doi.org/10.1016/S0039-6028\(03\)00929-4](http://dx.doi.org/10.1016/S0039-6028(03)00929-4)
- Blott, S. J., Pye, K., 2008. Particle shape: a review and new methods of characterization and classification. *Sedimentology* 55 (1), 31–63.
- Bogdanovičius, A., 2010. Fizikos pagrindai inžinerijoje, 1 dalis: vadovėlis [Fundamentals of Physics Engineering, Part 1: Handbook]. Vilnius, Technika, 340 pp. [In Lithuanian].

- Calvetti, F., 2008. Discrete modelling of granular materials and geotechnical problems. *European Journal of Environmental and Civil Engineering* 12 (7–8), 951–965. <http://dx.doi.org/10.1080/19648189.2008.9693055>
- Cavarretta, I., 2009. The influence of particle characteristics on the engineering behavior of granular materials. PhD thesis. London, London Imperial College, 420 pp.
- CEGEO, Saint-Cyr, B., Szarf, K., Voivret, C., Azéma, E., Richefeu, V., Delenne, J.–Y., Combe, G., Noguier-Lehon, C., Villard, P., Sornay, P., Chaze M., Radjai, F., 2012. Particle shape dependence in 2D granular media, *EPL (Europhysics Letters)* 98 (4), 44008.
- Charpentier, I., Sarocchi, D., Rodriguez Sedano, L. A. 2013. Particle shape analysis of volcanic clast samples with the Matlab tool MORPHEO. *Computers & Geosciences* 51, 172–181. <http://dx.doi.org/10.1016/j.cageo.2012.07.015>
- Chen, Y., Zhou, Q., 2012. A scale–adaptive DEM for multi-scale terrain analysis. *International Journal of Geographical Information Science* (2012), 1–20.
- Cho, G., Dodds, J., Santamarina, J., 2006. Particle shape effects on packing density, stiffness and strength: natural and crushed sands. *Journal of Geotechnical and Geoenvironmental Engineering* 132 (5), 591–602. [http://dx.doi.org/10.1061/\(ASCE\)1090-0241-\(2006\)132:5\(591\)](http://dx.doi.org/10.1061/(ASCE)1090-0241-(2006)132:5(591))
- Cundall, P. A., Strack, O. D. L., 1979. A discrete numerical model for granular assemblies. *Geotechnique* 29, 47–65. <http://dx.doi.org/10.1680/geot.1979.29.1.47>
- Dundulis, K., Gadeikis, S., Gadeikytė, S., Račkauskas, V., 2006. Sand soils of Lithuanian coastal area and their geotechnical properties. *Geologija* 53, 47–51.
- Dundulis, K., Gadeikis, S., Ignatavičius V., 2004. Kvartero nuogulų inžinerinių geologinių sąlygų formavimasis [Engineering geological conditions formation of Quaternary sediments]. Lietuvos gelmių raida ir išteklių. Spec. “Litosferos” leidinys, Vilnius, 318–331. [In Lithuanian].
- Fakhri, M., Kheiry, P. T., Mirghasemi, A. A., 2012. Modeling of permanent deformation characteristics of SMA mixtures using discrete element method. *Road Materials and Pavement Design* 13 (1), 67–84. <http://dx.doi.org/10.1080/14680629.2011.644080>
- Geng, Y., Yu, H. S., McDowell, G. R., 2012. Discrete element modelling of cavity expansion and pressuremeter test. *Geomechanics and Geoengineering: An International Journal* 8 (3), 179–190.
- Gadeikis, S., Repečka, M., 1999. Geotechnical properties of the Baltic Sea bottom sediments (Lithuanian near shore zone). *Baltica Special Publication* 12, 11–14.
- Gudelis, V., 1992. The Baltic: Sea and Coasts. Contribution of Lithuanian scientists. *Science, Arts and Lithuania* 2–3, 10–18.
- Gulbinskas, S., Trimonis, E., 1999. Distribution and composition of bottom sediments on the underwater slope at the Lithuanian coast of the Baltic Sea. *Baltica Special Publication* 12, 32–37.
- Yohannes, B., Tan, D., Khazanovich, L., Hill, K. M., 2013. Mechanistic modelling of tests of unbound granular materials. *International Journal of Pavement Engineering* (2013), 1–15.
- Jasevičius, R., Tomas, J., Kačianauskas, R., 2011. Simulation of normal impact of ultrafine silica particle on substrate. *Particulate Science and Technology: An International Journal* 29 (2), 107–126. <http://dx.doi.org/10.1080/02726351.2010.511662>
- Kavrus, A., Skuodis, Š., 2012. Smėlinių gruntų morfologinių parametrų nustatymas [Investigation of morphological parameters for sand soil]. In *Proceedings of the 15th Conference for Junior Researchers “Science – Future Lithuania”*, 22–24 May, Vilnius, Lithuania, 1–8. [In Lithuanian].
- Khanal, M., Tomas, J., 2008. Interparticle collision of particle composites–finite and discrete element simulations. *Particulate Science and Technology: An International Journal* 26 (5), 460–466. <http://dx.doi.org/10.1080/02726350802367720>
- Krugel-Emden, H., Rickelt, S., Wirtz, S., Scherer, S., 2008. A study on the validity of the multi-sphere Discrete Element Method. *Powder Technology* 188, 153–165. <http://dx.doi.org/10.1016/j.powtec.2008.04.037>
- Krumbein, W., Slos, L., 1951. Stratigraphy and Sedimentation. A series of books in geology. San Francisco, W. H. Freeman and Co, 497 pp.
- Lewandowska, J., Pilawski, M., 2012. Experiments and micromechanical modelling of a composite geomaterial. *European Journal of Environmental and Civil Engineering* 16 (2), 121–140. <http://dx.doi.org/10.1080/19648189.2012.667694>
- Lim, W. L., McDowell, G. R., 2008. A limit analysis of the kinematics of void collapse using the discrete element method. *Geomechanics and Geoengineering: An International Journal* 3 (1), 41–58.
- Lin, J., Wu, W., 2012. Numerical study of miniature penetrometer in granular material by discrete element method. *Philosophical Magazine* 92 (28–30), 3474–3482. <http://dx.doi.org/10.1080/14786435.2012.706373>
- LST EN ISO 14688–2:2007. Geotechniniai tyrinėjimai ir bandymai. Gruntų atpažintis ir klasifikavimas. 2 dalis: Klasifikavimo principai (ISO 146882–2:2004) [Geotechnical investigation and testing – Identification and classification of soil – Part 2: Principles for classification (ISO 146882–2:2004)]. LSD, 14 pp.
- Luding, S., 2008. Introduction to discrete element methods. *European Journal of Environmental and Civil Engineering* 12 (7–8), 785–826. <http://dx.doi.org/10.1080/19648189.2008.9693050>
- Markauskas, D., Kačianauskas R., 2006. Compacting of particles for biaxial compression test by the discrete element method. *Journal of Civil Engineering and Management* 12 (2), 153–161.
- Modenese, C., Utili, S., Houlsby, G. T., 2012. A numerical investigation of quasi–static conditions for granular media. In *Proceedings of the International Symposium on Discrete Element Modelling of Particulate Media*, University of Birmingham, 29–30 March 2012. <http://dx.doi.org/10.1039/9781849735032-00187>

- Mollon, G., Zhao, J., 2013. Generating realistic 3D sand particles using Fourier descriptors. *Granular Matter* 15 (1), 95–108. <http://dx.doi.org/10.1007/s10035-012-0380-x>
- Montenegro Ríos, A., Sarocchi, D., Nahmad-Molinari, Y., Borselli, L., 2013. Form From Projected Shadow (FFPS): An algorithm for 3D shape analysis of sedimentary particles. *Computers and Geosciences* 60, 98–108. <http://dx.doi.org/10.1016/j.cageo.2013.07.008>
- Prisco, C., Galli, A., 2011. Mechanical behaviour of geocased sand columns: small scale experimental tests and numerical modelling. *Geomechanics and Geoengineering: An International Journal* 6 (4), 251–263.
- Prušinskienė, S., 2012. Smėlio gruntų ypatumai ir jų tyrimo metodai. Mokomoji knyga [Sand soil peculiarities and investigation methods. Instructional book], Vilnius, Technika, 183 pp. [In Lithuanian]. <http://dx.doi.org/10.3846/1314-S>
- Renouf, M., Dubois, F., Alart, P., 2006. Numerical investigations of fault propagation and forced-fold using a non smooth discrete element method. *European Journal of Computational Mechanics/Revue Européenne de Mécanique Numérique* 15 (5), 549–570.
- Repečka, M., 1999. Quaternary sediments on the bottom surface of the south-eastern Baltic Sea. *Baltica Special Publication* 12, 93–98.
- Roussillon, T., Piégay, H., Sivignon, I., Tougne, L., Lavigne, F., 2009. Automatic computation of pebble roundness using digital imagery and discrete geometry. *Computers and Geosciences* 35, 1992–2000. <http://dx.doi.org/10.1016/j.cageo.2009.01.013>
- Safronov, D., Nikrityuk, P., Meyer, B., 2012. Fixed-grid method for the modelling of unsteady partial oxidation of a spherical coal particle. *Combustion Theory and Modelling* 16 (4), 589–610. <http://dx.doi.org/10.1080/13647830.2011.643242>
- Singh, D., Zaman, M., Commuri, S., 2012. Inclusion of aggregate angularity, texture and form in estimating dynamic modulus in asphalt mixtures. *Road Materials and Pavement Design* 12 (2), 327–344. <http://dx.doi.org/10.1080/14680629.2011.650088>
- Skuodis, Š., Norkus, A., Tumonis, L., Amšiejus, J., Akšamitauskas, Č., 2013. Experimental and numerical investigation of sand compression peculiarities. *Journal of Civil Engineering and Management* 19 (1), 78–85. <http://dx.doi.org/10.3846/13923730.2013.756164>
- Statkus, T., Martinkus, V., 2013. The results of correlation between cone tip resistance, push-In pressure load cells and a compression device, *Science – Future of Lithuania* 5 (5), 525–529. [In Lithuanian].
- STIMAN. 2010. Structural image analysis. Moscow State University. Moscow, 156 pp.
- Tafesse, S., Robison Fernlund, J. M., Sun, W., Bergholm, F., 2013. Evaluation of image analysis methods used for quantification of particle angularity. *Sedimentology* 60, 1100–1110. <http://dx.doi.org/10.1111/j.1365-3091.2012.01367.x>
- Tong, F., Yin, J. H., 2011. Nonlinear creep and swelling behavior of bentonite mixed with different sand contents under oedometer condition. *Marine Georesources and Geotechnology* 29 (4), 346–363. <http://dx.doi.org/10.1080/1064119X.2011.560824>
- Tordesillas, A., Zhang, J., Behringer, R., 2009. Buckling force chains in dense granular assemblies: physical and numerical experiments. *Geomechanics and Geoengineering: An International Journal* 4 (1), 3–16.
- Tumonis, L., Kačianauskas, R., Norkus, A., Žilionienė, D., 2012. Comparison study of spherical and multi-spherical particles under cyclic uniaxial compression. *Journal of Civil Engineering and Management* 18 (4), 537–545. <http://dx.doi.org/10.3846/13923730.2012.702127>
- Vittorias, E., Kappl, M. Butt, H. J., 2010. Studying mechanical microcontacts of fine particles with the quartz crystal microbalance. *Powder Technology* 203 (2010), 489–502. <http://dx.doi.org/10.1016/j.powtec.2010.06.011>
- Wille Geotec Group, 2010. Universal oedometer test device ADS 1/3. Göttingen, Germany, 36 pp.
- Wu, J., Collop, A., McDowell, G., 2009. Discrete element modelling of monotonic compression tests in an idealised asphalt mixture. *Road Materials and Pavement Design* 10 (suppl.), 211–232.
- Zhu, H. P., Zhou, Z. Y., Yang, R. Y., Yu, A. B., 2008. Discrete particle simulation of particulate systems: A review of major applications and findings. *Chemical Engineering Science* 63 (23), 5728–5770. <http://dx.doi.org/10.1016/j.ces.2008.08.006>